Second harmonic generation of violet light in femtosecond-laser-inscribed BiB_3O_6 cladding waveguides

Yuechen Jia[1], J. R. Vázquez de Aldana[2], Qingming Lu[3], D. Jaque[4], and Feng Chen[1,*]

[1]*School of Physics, State Key Laboratory of Crystal Materials, and Key Laboratory of Particle Physics and Particle Irradiation (Ministry of Education), Shandong University, Jinan 250100, China*
[2]*Laser Microprocessing Group, Universidad de Salamanca, Salamanca 37008, Spain*
[3]*School of Chemistry and Chemical Engineering, Shandong University, Jinan 250100, China*
[4]*Fluorescence Imaging Group, Departamento de Física de Materiales, Facultad de Ciencias, Universidad Autónoma de Madrid, Madrid 28049, Spain*
[*]*drfchen@sdu.edu.cn*

Abstract: Depressed cladding waveguide structures have been fabricated in BiB_3O_6 nonlinear crystal by using femtosecond (fs) laser inscription. The nonlinear properties of original BiB_3O_6 crystal have been well preserved within the waveguide volume. Under 800 nm continuous wave laser pumping, the guided-wave second harmonic generation of violet light at 400 nm has been realized, with a maximum power of ~1.05 mW and a conversion efficiency of ~0.98%/W.

OCIS codes: (230.7370) Waveguides; (190.4390) Nonlinear optics, integrated optics; (140.3390) Laser materials processing.

References and links

1. E. J. Murphy, *Integrated Optical Circuits and Components: Design and Applications* (Marcel Dekker, 1999).
2. C. Grivas, "Optically pumped planar waveguide lasers, Part I: Fundamentals and fabrication techniques," Prog. Quantum Electron. **35**(6), 159–239 (2011).
3. F. Chen, "Micro-and submicrometric waveguiding structures in optical crystals produced by ion beams for photonic applications," Laser Photon. Rev. **6**(5), 622–640 (2012).
4. D. N. Nikogosyan, *Nonlinear Optical Crystals: A Complete Survey* (Springer, 2005).
5. M. Ghotbi and M. Ebrahim-Zadeh, "Optical second harmonic generation properties of BiB_3O_6," Opt. Express **12**(24), 6002–6019 (2004).
6. V. Petrov, M. Ghotbi, O. Kokabee, A. Esteban-Martin, F. Noack, A. Gaydardzhiev, I. Nikolov, P. Tzankov, I. Buchvarov, K. Miyata, A. Majchrowski, I. V. Kityk, F. Rotermund, E. Michalski, and M. Ebrahim-Zadeh, "Femtosecond nonlinear frequency conversion based on BiB_3O_6," Laser Photonics Rev. **4**(1), 53–98 (2010).
7. F. Chen, H. Hu, K. M. Wang, B. Teng, J. Y. Wang, Q. M. Lu, and D. Y. Shen, "Formation of a planar optical waveguide by mega-electron-volt He^+ and P^+ ions implanted in a BiB_3O_6 crystal," Opt. Lett. **26**(24), 1993–1995 (2001).
8. L. Wang, F. Chen, X. L. Wang, K. M. Wang, Q. M. Lu, and H. J. Ma, "Formation of planar waveguide in BiB_3O_6 crystal by MeV carbon implantation," Nucl. Instr. and Meth. B **266**(6), 899–903 (2008).
9. S. J. Beecher, R. R. Thomson, D. T. Reid, N. D. Psaila, M. Ebrahim-Zadeh, and A. K. Kar, "Strain field manipulation in ultrafast laser inscribed BiB_3O_6 optical waveguides for nonlinear applications," Opt. Lett. **36**(23), 4548–4550 (2011).
10. Y. C. Jia, J. R. Vázquez de Aldana, C. Romero, Y. Y. Ren, Q. M. Lu, and F. Chen, "Femtosecond-laser-inscribed BiB_3O_6 nonlinear cladding waveguide for second-harmonic generation," Appl. Phys. Express **5**(7), 072701 (2012).
11. R. R. Gattass and E. Mazur, "Femtosecond laser micromachining in transparent materials," Nat. Photonics **2**(4), 219–225 (2008).
12. R. Osellame, G. Cerullo, and R. Ramponi, *Femtosecond Laser Micromachining: Photonic and Microfluidic Devices in Transparent Materials* (Springer, 2012).
13. F. Chen and J. R. Vázquez de Aldana, "Optical waveguides in crystalline dielectric materials produced by femtosecond laser micromachining," Laser Photonics Rev. DOI: 10.1002/lpor.201300025 (2013).
14. K. Sugioka and Y. Cheng, "Femtosecond laser processing for optofluidic fabrication," Lab Chip **12**(19), 3576–3589 (2012).

#193379 - $15.00 USD Received 9 Jul 2013; revised 1 Aug 2013; accepted 4 Aug 2013; published 9 Aug 2013

15. K. M. Davis, K. Miura, N. Sugimoto, and K. Hirao, "Writing waveguides in glass with a femtosecond laser," Opt. Lett. **21**(21), 1729–1731 (1996).
16. S. Juodkazis, V. Mizeikis, and H. Misawa, "Three-dimensional microfabrication of materials by femtosecond laser for photonics applications," J. Appl. Phys. **106**(5), 051101 (2009).
17. M. Ams, G. D. Marshall, P. Dekker, J. A. Piper, and M. J. Withford, "Ultrafast laser written active devices," Laser Photonics Rev. **3**(6), 535–544 (2009).
18. J. Choi, M. Bellec, A. Royon, K. Bourhis, G. Papon, T. Cardinal, L. Canioni, and M. Richardson, "Three-dimensional direct femtosecond laser writing of second-order nonlinearities in glass," Opt. Lett. **37**(6), 1029–1031 (2012).
19. J. T. Lin, S. J. Yu, Y. G. Ma, W. Fang, F. He, L. L. Qiao, L. M. Tong, Y. Cheng, and Z. Z. Xu, "On-chip three-dimensional high-Q microcavities fabricated by femtosecond laser direct writing," Opt. Express **20**(9), 10212–10217 (2012).
20. J. R. Grenier, L. A. Fernandes, and P. R. Herman, "Femtosecond laser writing of optical edge filters in fused silica optical waveguides," Opt. Express **21**(4), 4493–4502 (2013).
21. J. Burghoff, S. Nolte, and A. Tünnermann, "Origins of waveguiding in femtosecond laser-structured $LiNbO_3$," Appl. Phys., A Mater. Sci. Process. **89**(1), 127–132 (2007).
22. L. B. Fletcher, J. J. Witcher, N. Troy, S. T. Reis, R. K. Brow, and D. M. Krol, "Direct femtosecond laser waveguide writing inside zinc phosphate glass," Opt. Express **19**(9), 7929–7936 (2011).
23. R. Mary, S. J. Beecher, G. Brown, R. R. Thomson, D. Jaque, S. Ohara, and A. K. Kar, "Compact, highly efficient ytterbium doped bismuthate glass waveguide laser," Opt. Lett. **37**(10), 1691–1693 (2012).
24. G. A. Torchia, A. Rodenas, A. Benayas, E. Cantelar, L. Roso, and D. Jaque, "Highly efficient laser action in femtosecond-written Nd:yttrium aluminum garn et ceramic waveguides," Appl. Phys. Lett. **92**(11), 111103 (2008).
25. J. Siebenmorgen, K. Petermann, G. Huber, K. Rademaker, S. Nolte, and A. Tunnermann, "Femtosecond laser written stress-induced Nd:$Y_3Al_5O_{12}$ (Nd:YAG) channel waveguide laser," Appl. Phys. B **97**(2), 251–255 (2009).
26. A. M. Streltsov, "Femtosecond-laser writing of tracks with depressed refractive index in crystals," Proc. SPIE **4941**, 51–57 (2003).
27. A. Okhrimchuk, V. Mezentsev, A. Shestakov, and I. Bennion, "Low loss depressed cladding waveguide inscribed in YAG:Nd single crystal by femtosecond laser pulses," Opt. Express **20**(4), 3832–3843 (2012).
28. D. G. Lancaster, S. Gross, H. Ebendorff-Heidepriem, K. Kuan, T. M. Monro, M. Ams, A. Fuerbach, and M. J. Withford, "Fifty percent internal slope efficiency femtosecond direct-written Tm^{3+}:ZBLAN waveguide laser," Opt. Lett. **36**(9), 1587–1589 (2011).
29. N. N. Dong, F. Chen, and J. R. Vázquez de Aldana, "Efficient second harmonic generation by birefringent phase matching in femtosecond laser inscribed KTP cladding waveguides," Phys. Status Solidi: rrl **6**(7), 306–308 (2012).
30. M. Thorhauge, J. L. Mortensen, P. Tidemand-Lichtenberg, and P. Buchhave, "Tunable intra-cavity SHG of CW Ti:Sapphire lasers around 785 nm and 810 nm in BiBO-crystals," Opt. Express **14**(6), 2283–2288 (2006).

1. Introduction

In integrated micro-photonic devices, nonlinear optical guiding structures are attracting a great attention owing to the combination of the original nonlinear properties of substrates and the compact confinement of light propagation within considerably compressed volumes [1–3]. As one of the most intriguing nonlinear materials for effective frequency conversion, the monoclinic bismuth borate (BiB_3O_6 or BIBO) crystal is of special relevance owing to its remarkable large nonlinear optical coefficient (d_{eff} = 3.2 pm/V) as well as high damage threshold (~5 GW/cm^2) [4]. The second harmonic generation (SHG) from visible till UV spectral ranges can be achieved in BiB_3O_6 via birefringent phase matching (BPM) mechanism [5,6]. Taking the advantages of the nonlinear features of BiB_3O_6 crystal and compact geometry of waveguides, promising micro-photonic components may be fabricated for efficient frequency conversion. As of yet, waveguide structures in BiB_3O_6 crystals fabricated by ion implantation and fs laser inscription have been reported [7–10], and efficient SHG of green light has been realized [10]. Nevertheless, there has been no report on SHG of violet light in BiB_3O_6 waveguides.

Tightly focused fs laser pulses could directly modify the optical properties of the transparent materials at both micro and sub-micro scales, based on the structural modifications induced at the focal spot and in its surroundings [11–14]. Benefiting from this feature, fs laser inscription technique has become a powerful and unique method for the construction of three-dimensional (3D) guiding structures inside versatile transparent materials [9–29], since the pioneering work by Davis *et al.* in 1996 [15]. Basically, the fs-

#193379 - $15.00 USD Received 9 Jul 2013; revised 1 Aug 2013; accepted 4 Aug 2013; published 9 Aug 2013

laser-written waveguides could be classified into directly written structures (Type I waveguides with single line writing) [21–23], stress-induced waveguides (Type II waveguides with double-line filaments) [9,21,24,25], and cladding waveguides (structures usually with large area cross sections) [10,26–29]. In this last fabrication strategy, the waveguide core is located in the section surrounded by multiple low-index damaged tracks induced by the fs-laser inscription. Such a configuration was firstly proposed by Streltsov in 2003 [26]. Compared to the first two types of guiding geometries, the cladding waveguides could be manufactured with arbitrarily designed cross sections without requiring complex sample manipulation (such as rotation). Particularly, the scales of the cladding waveguide cross section could be designed to match the diameters of the commercially available multimode fibers (with diameters of 100-400 μm), which in principle offers an opportunity to construct efficient fiber-waveguide integrated photonic chips with low costs. In addition, the cladding structures seem to be much efficient and well-matched for nonlinear crystals because the large-dimension waveguide volumes may offer good guidance for any polarization direction in the cross-sectional plane, which guarantees birefringent frequency doubling, under either Type I or Type II PM configuration, efficiently realized. Recently, we have reported the fabrication of nonlinear cladding waveguides in $KTiOPO_4$ and BiB_3O_6 crystals and the realization of SHG under birefringent PM configuration for 1064→532 nm [10,29]. In this work, we report on the fabrication of the BiB_3O_6 cladding waveguide and its SHG features for the 800→400 nm SHG of violet light.

2. Experiments in details

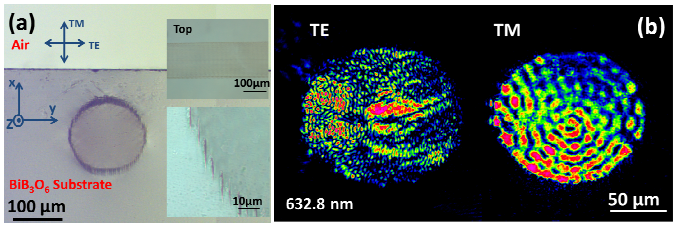

Fig. 1. (a) Optical transmission microscopy image of the cross section of the BiB_3O_6 cladding waveguide with a diameter of 150 μm. The insets depict the top view of the waveguide and the magnification of a section of the waveguide contour. And (b) the near-field intensity distributions of the TE and TM modes for the cladding waveguide at a wavelength of 632.8 nm.

The optically polished BiB_3O_6 crystal sample used in this work was cut into wafers with dimensions of 7(z) × 5(y) × 2(x) mm^3 along the phase matching direction for efficient 800 to 400 nm Type I SHG (i.e. $e^{\omega} + e^{\omega} \rightarrow o^{2\omega}$) in the *y*-*z* plane ($\theta = 151.2°$, $\varphi = 90°$). The depressed cladding waveguide structures were fabricated by utilizing the laser facilities at the Universidad de Salamanca. An amplified Ti:Sapphire laser system (Spitfire, Spectra Physics, USA), generating linearly-polarized 120 fs pulses at a central wavelength of 800 nm (with 1 kHz repetition rate and 1 mJ maximum pulse energy), was employed as laser source. We used a calibrated neutral density filter, a half-wave plate and a linear polarizer to finely control the value of the pulse energy used to irradiate the sample. A 40 × microscope objective (N.A. = 0.4) was utilized to focus the laser beam at a certain depth beneath the largest sample surface (dimensions of 7 × 5 mm^2), and several tests at different pulse energies and scanning velocities were performed. Optical microscopy (in transmission mode) was used to evaluate the damage tracks produced in the sample and the final irradiation parameters were fixed to 0.21 μJ of pulse energy. During the irradiation process the sample was placed in a computer controlled motorized 3-axes stage, moving at a constant speed of 700 μm/s in the direction perpendicular to the laser beam polarization. The writing direction was carefully aligned with the 5-mm long edge of the sample. Consequently, a damage track

#193379 - $15.00 USD Received 9 Jul 2013; revised 1 Aug 2013; accepted 4 Aug 2013; published 9 Aug 2013

along the sample was produced. For the chosen polarization (y-direction), no evidence of multiple focusing due to birefringence was found in the crystal. The optimum values of velocity and pulse energy were chosen as a compromise between producing a large enough damage in the laser tracks (large index contrast) and minimizing the formation of cracks in the sample. Many parallel scans (with ~4 μm lateral separation between adjacent damage tracks) were performed at different depths of the sample (from bottom to top in order to avoid the shielding of the incident pulses by the previously written damage tracks) to inscribe the cladding waveguide structure with a diameter of 150 μm. The microscope images of cross section of the resulting structure in the BiB_3O_6 can be seen in Fig. 1(a). The insets depict the top view of the cladding waveguide and the magnification of a section of the waveguide contour (i.e. the damage tracks).

To experimentally characterize the modal profiles of the cladding waveguide, we arranged an end-face coupling experiment by using a He-Ne laser at wavelength of 632.8 nm. The resulting distributions are shown in Fig. 1(b). One can find that the cladding waveguide structure support multimode guidance in any transverse direction (i.e. for both TE and TM polarizations), just as expected. We believe the difference between TE and TM guiding modes is mostly due to the birefringence of the BiB_3O_6 substrate. As for the multimode distributions, which can be well understood in terms of the large size of the structures compared to the test wavelength (632.8 nm), just like shown in previous works [10]. In addition, we also performed the waveguide loss measurement at 632.8 nm, by considering the transmittance and reflectivity of the optical elements used in the experiment setup as well as the Fresnel reñection loss at the end facets (in our case, the value is about 0.4 dB in the interface of the waveguide end face and the air) into account. The insertion loss of the cladding was estimated to be 1.3 ± 0.3 dB/cm. A difference of 0.6 dB here was found between the TE and TM polarizations (the TE polarized light shows higher insertion losses than TM modes).

In order to investigate the preservation of original nonlinear response at the fabricated waveguide volume after fs laser inscription procedure, we performed the μ-SH measurement by employing a home-made confocal fluorescence microscope at the Fluorescence Imaging Group (Universidad Autónoma de Madrid, Spain). A single-mode fiber coupled mode-locked Ti:Sapphire laser (Millenia, Spectra Physics) providing 100 fs, 800 nm wavelength pulses at a repetition rate of 80 MHz. The 800 nm laser beam at the exit of the single mode fiber was collimated and focused into the sample by a 100 × microscope objective with a NA of 0.9. The subsequent backscattered second harmonic radiation at 400 nm was collected with the same objective and, after passing through a set of filters, lenses and pinholes, it was spectrally analyzed by a high resolution spectrometer. The sample was mounted on an *x*-*y* motorized stage with the spatial resolution of 100 nm so that the position of the 800 nm spot in respect to the waveguide structure was automatically controlled. In this work the methodology employed for SH imaging of the waveguides consisted on the scanning of the 800 nm laser spot over the waveguide cross section by performing 1 μm steps over a 400 μm^2 area. The 800 nm laser power was kept below 20 mW in order to avoid surface damage and the integration time used for the acquisition of the SH emission was set to 1 s per point.

The experiment for characterizing the nonlinear performance of the fs-fabricated waveguide was implemented with an end-face coupling system. For the SHG of BiB_3O_6 cladding waveguide, a continuous-wave (cw) polarized laser beam at a wavelength of 800 nm generated from a tunable Ti:Sapphire laser (Coherent MBR 110), acting as the fundamental wave, was coupled into the waveguide by a convex lens with focal length of f = 25 mm. The polarization of the fundamental wave was controlled by a half-wave plate. The light emerging from the output end face of the waveguide was captured by employing a microscope objective lens with a NA of 0.4. And the generated SH light was separated from the residual fundamental laser beam by utilizing a dichroic mirror with transmission of ~70%

#193379 - $15.00 USD Received 9 Jul 2013; revised 1 Aug 2013; accepted 4 Aug 2013; published 9 Aug 2013

at ~400 nm and reflectivity >99% at ~800 nm, and then detected by a spectrometer, a visible CCD camera as well as a powermeter.

3. Results and discussion

The relative refractive index reductions (Δn) at the waveguide counter (i.e. the locations of fs-laser damaged tracks) with respect to the bulk was estimated by using the equation $\Delta n = \sin^2 \Theta_m / (2n)$. In this equation, n is the substrate refractive index at 632.8 nm, and Θ_m is the maximum beam divergence of the light entering or leaving the waveguide, which was measured by rotating a cubic K9 glass before the incident light coupling into the waveguide structure. According to the measured Θ_m value, the effective refractive index changes possess the order of 10^{-3}. This value is in good agreement with our previous work [10].

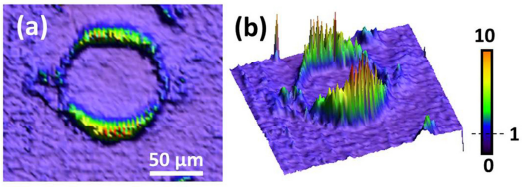

Fig. 2. (a) 2D and (b) 3D confocal μ-SH cross-sectional mappings obtained from the end face of the fs laser inscribed BiB_3O_6 cladding waveguide.

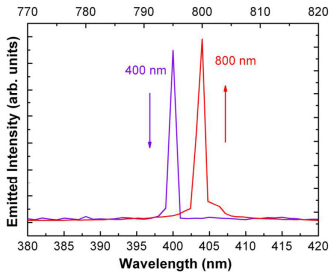

Fig. 3. Normalized spatial intensity distributions of the 800 nm fundamental wave (red) and 400 nm SH wave (violet) from the BiB_3O_6 cladding waveguide.

Figure 2 depicts 2D and 3D confocal μ-SH images of the waveguide cross-section as obtained for the end face of the cladding waveguide. As can be observed, the nonlinear properties of the BiB_3O_6 crystal have not been modified in the waveguide volume during fs-laser inscription, but enhanced markedly at the waveguide contour (about 8-10 times the emitted intensity of bulk material), where the BiB_3O_6 network is simultaneously damaged, compressed and disordered by fs laser irradiation. The origin of this local SH back-scattered intensity enhancement could be explained in terms of a combination of two effects. On one hand, damage volumes increase the local density of scattering points so that the back-scattering efficiency and the back scattered SH Intensity are both enhanced (i.e., the measured enhancement of the back-scattered signals and back-scattering efficiency in those areas is due to the larger-density defects, which act as scattering centers and reflecting back the SH radiation). The second effect is that damage volumes are very likely characterized by a high density of extended defects and micro-cracks. The original material in the surroundings of micro-cracks and defects has an additional source of non-linearity since the systems increases their level of asymmetry. This could, in turns, increase the local value of nonlinear coefficients and, hence, the collected back-scattered SH intensity.

The normalized spectra of fundamental wave and SH waveguide laser modes as obtained in end-coupling experiments are depicted in Fig. 3. As can be seen, the emission lines of fundamental wave and SH violet laser are peaked at 800 nm and 400 nm, respectively,

#193379 - $15.00 USD Received 9 Jul 2013; revised 1 Aug 2013; accepted 4 Aug 2013; published 9 Aug 2013

clearly depicts the nonlinear process of SHG in BiB_3O_6 waveguides. The frequency doubling laser at 400 nm was found along TM polarization, which is perpendicular to the fundamental wave polarizing orientation (TE polarization), i.e. $TE^{\omega} + TE^{\omega} \rightarrow TM^{2\omega}$ frequency conversion, corresponding to the bulk Type I (i.e. $e^{\omega} + e^{\omega} \rightarrow o^{2\omega}$) birefringent PM.

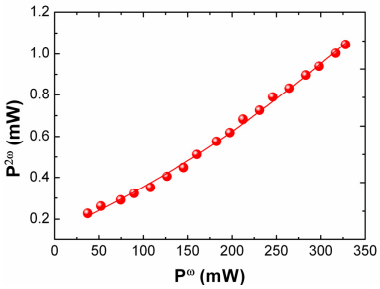

Fig. 4. SHG output power versus the fundamental pump power of the BiB_3O_6 cladding waveguide under cw laser pump. The solid lines represent the fit of the experimental data.

Figure 4 depicts the generated SH wave power at 400 nm as a function of the fundamental pump power at 800 nm from the fs inscribed BiB_3O_6 cladding waveguide. As it can be observed, the maximum violet laser output power was measured to be ~1.05 mW when the fundamental laser power was around 328 mW, corresponding to a SH conversion efficiency of approximately ~0.32% (normalized value of ~0.98%/W), which is slightly larger than the reported SH conversion efficiencies for green laser in BiB_3O_6 waveguides (~0.015%/W and 0.75%/W for fs laser fabricated Type II stress-induced and depressed cladding waveguides in BiB_3O_6 crystals, respectively) [9,10]. However, this value is still on a relatively low level when compared to the conversion efficiency of BiB_3O_6 bulk material pumped by Ti:sapphire laser (which is approximately 1.82% at 405 nm) [30], we believe that to be partly due to the high attenuation of the waveguide structure as well as the low pumping power. In addition to this, the non-single mode of the guidance in the waveguide may also an important factor leading to the reduction.

4. Summary

The 800→400 nm SHG has been successfully demonstrated in a BiB_3O_6 cladding waveguide with a diameter of 150 μm fabricated by fs laser inscription technique. The μ-SH images of the waveguide's cross section have revealed that the nonlinear response of original BiB_3O_6 crystal have been well preserved within the waveguide. We have obtained output SH powers up to ~1.05 mW with a conversion efficiency of ~0.32% (normalized value of ~0.98%/W) at 400 nm when the guiding structure was optically excited by a 300 mW 800 nm laser beam. The SHG performance indicates potential applications of the fs laser inscribed BiB_3O_6 cladding waveguides as promising integrated frequency converters for violet light.

Acknowledgments

This work is supported by the National Natural Science Foundation of China (No. 11274203), the Spanish Ministerio de Ciencia e Innovación (MICINN) through Consolider Program SAUUL CSD2007-00013 and projects FIS2009-09522 and MAT2010-16161, and Junta de Castilla y León (Project SA086A12-2). Supports from the Centro de Láseres Pulsados (CLPU) and Comunidad Autonoma de Madrid (S2009/ MAT-1756) are also acknowledged.

#193379 - $15.00 USD Received 9 Jul 2013; revised 1 Aug 2013; accepted 4 Aug 2013; published 9 Aug 2013